Extended Abstracts of the 1993 International Conference on Solid State Devices and Materials, Makuhari, 1993, pp. 464-466

Modeling of the Hole Current Caused by Fowler-Nordheim Tunneling through Thin Oxides

Gertjan Hemink, Tetsuo Endoh, and Riichiro Shirota

Toshiba Research and Development Center
ULSI Research Laboratories
1, Komukai Toshiba-cho, Saiwai-ku, Kawasaki 210, Japan

A new model for the substrate hole current that occurs during Fowler-Nordheim (FN) stress of thin oxides is proposed. The probability that a hole is emitted in the oxide is described by an empirical relation that is a function of the effective barrier height and the average energy of the electrons arriving at the anode. The results obtained with the model are in very good agreement with the measurements for oxides within a thickness range of 5.5 to 12.5 nm.

I. Introduction

It has been suggested by several authors[1-3] that the substrate hole current, which occurs under Fowler-Nordheim stress with a positive gate voltage, is caused by hot hole injection from the anode interface. However, others assumed that impact ionization in the oxide is the main cause of the hole current[4,5]. The hole current also occurs for oxides with a thickness of 8.5 nm, where the energy that can be acquired by the electrons is less than the oxide band gap. Therefore, it has been concluded in [2,6] that impact ionization in the oxide could not be the only mechanism for the hole current generation. The model for the hole current presented in this letter is based on the surface plasmon model[7], thus assuming hot hole injection from the anode. However, the model used in [7] is complicated and requires knowledge about the electron energy distribution function. Moreover, it has been assumed in [7] that the electron energy distribution function reaches a field dependent steady state distribution that is independent of the oxide thickness. This assumption is not correct, at least not for the oxide thickness range discussed here, since the measurements presented here and in [1] clearly show a dependence on the oxide thickness. To take the effect of the oxide thickness into account, the new model proposed here is based on the average electron energy.

II. Model and experimental results

Figure 1 shows the band diagram and the hole injection mechanism that occurs during FN tunneling of electrons

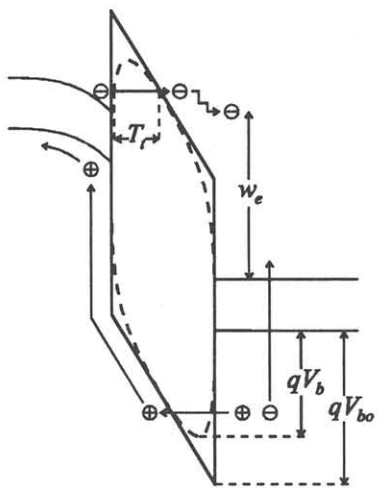

Fig. 1. Energy band diagram and the hole injection mechanism that occurs during Fowler-Nordheim tunneling.

from the inversion layer to the gate of a NMOS transistor. After tunneling through the potential barrier, the electrons will gain energy from the electric field in the oxide and will lose energy by various scattering mechanisms[8,9]. The hot electrons arriving at the anode will lose their energy by emitting surface plasmons. The emitted surface plasmons will decay via the excitation of electron/hole pairs and by the generation of both hot holes and electrons. The hot holes may be emitted over or tunnel through the potential barrier and contribute to the hole current. The computation of the average electron energy will be discussed in section II.1. Furthermore a model for the effective hole barrier height and the hole emission probability as a function of the

effective barrier height and the electron energy will be discussed in section II.2 and II.3 respectively.

II.1. The average electron energy

To compute the average energy of the electrons, the energy relaxation time approximation is used. This technique is widely used to compute the drift velocity and the average energy in silicon[10]. Assuming that the drift velocity in the oxide does not depend on the position in the oxide, only the equation for the average energy has to be solved and can be written as

$$\frac{d<w>}{dx} = qE_{ox} - \frac{(<w> - w_o)}{\lambda(<w>)} \qquad (1)$$

where $<w>$ the average electron energy, q the electronic charge, E_{ox} the electric field strength in the oxide, w_o $(1.5kT)$ the average energy in thermal equilibrium with k the boltzman constant, T the temperature, and $\lambda(<w>)$ the energy relaxation distance as a function of the average electron energy. This equation can be solved numerically and yields the average electron energy as a function of the position x in the oxide. The relaxation length $\lambda(<w>)$ can be determined from the static $<w>(E_{ox})$ characteristics by equation (1) with $d<w>/dx = 0$. These static characteristics can be computed by Monte-Carlo simulations or obtained from measurements[8,9]. Here, an empirical function for $\lambda(<w>)$ is used. This function is depicted in figure 2.a. Using this function the static $<w>(E_{ox})$ relation can be computed and is shown in figure 2.b. The resulting $<w>(E_{ox})$ is in good agreement with the results obtained by Monte-Carlo simulations[8].

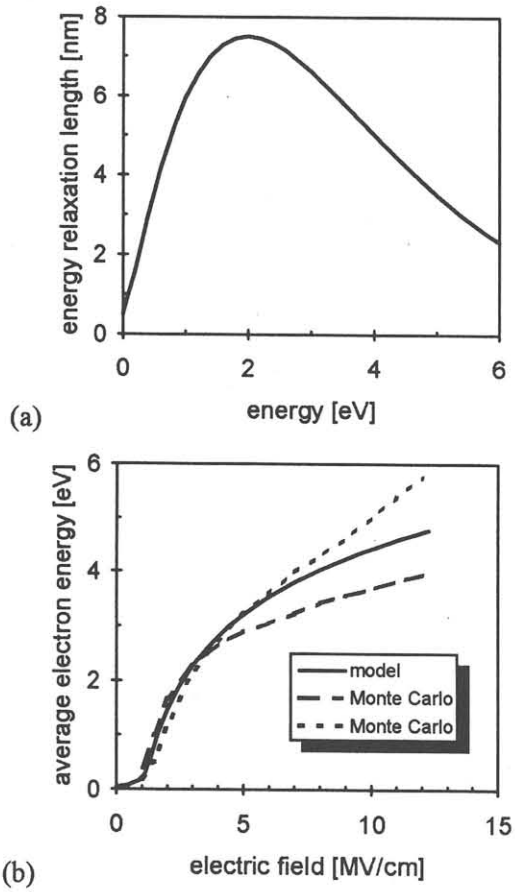

Fig. 2. The empirical function of the energy relaxation length $\lambda(<w>)$ as a function of the average electron energy in the oxide (a) and the average electron energy $<w>$ as a function of the electric field strength in the oxide under static conditions ($d<w>/dx = 0$) (b). The solid line corresponds with computations using the empirical $\lambda(<w>)$ expression. The dashed lines correspond with Monte-Carlo simulations described in [8]. Two different models, with and without the collision broadening effect, have been used in these Monte-Carlo simulations.

II.2. The effective barrier height

As for hot electron injection[11], the barrier height has to be corrected for the image force effect and an additional tunneling barrier lowering term has to be used to account for hot hole tunneling through the potential barrier. The uncorrected hole barrier height qV_{bo} is 4.7 eV[7]. The valence band potential is corrected for the image force effect and the barrier height qV_b can be easily derived from the computed valence band potential curve (see fig. 1). Including the additional barrier lowering term to account for hole tunneling, the effective barrier height can be written as

$$qV_{beff} = qV_b - \alpha E_{ox}^{2/3} \qquad (2)$$

where α is a fitting parameter.

II.3. The computation of the hole current

A part of the energy of the hot electrons arriving at the anode is lost for the generation of electron/hole pairs. It has been shown that, for oxide thicknesses in the range of 7.9-18.7 nm, every electron generates about 1.5 electron/hole pairs[12]. Assuming that the generation of one electron/hole pair requires the silicon bandgap energy, the energy that is available to generate hot carriers is given by

$$<w_h> = <w_e> - 1.5E_{gap} \qquad (3)$$

with $<w_e>$ the average energy of the electrons arriving at the anode and E_{gap} the silicon bandgap energy (1.1 eV). A part of this energy will be transferred to the generated holes, therefore the average energy of the hot holes is assumed to be linear dependent on $<w_h>$.

After the computation of $<w_h>$, the hole current has to be related to this energy. For the modeling of hot electron gate currents, the Richardson equation has been often used[13]. In that equation, the emission probability

is a function of the average electron energy and the effective barrier height of the SiO_2 potential barrier. However, it has been shown that the Richardson equation overestimates the hot electron gate current for several orders of magnitude[14]. Therefore, the model used here is based on an empirical model for substrate hot electron injection[15]. The hole current density I_p is given by

$$I_p = 1.5 I_n P_e = 1.5 I_n \exp\left(-B_e \frac{qV_{beff}}{< w_h >}\right) \quad (4)$$

with P_e the emission probability, qV_{beff} the effective barrier height for holes and B_e a fitting parameter. In this equation $1.5I_n$ represents the number of holes available for emission, because every electron generates about 1.5 electron/hole pairs.

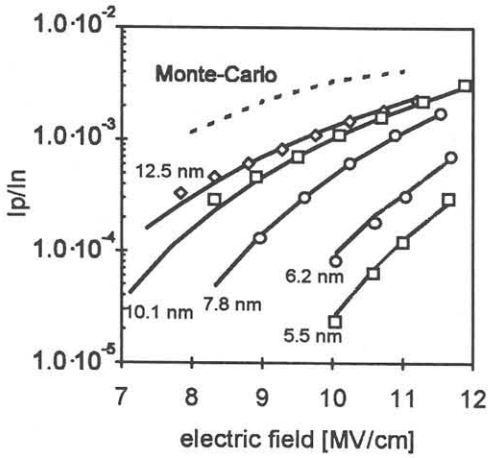

Fig. 3. Computed and measured I_p/I_n ratios for different oxide thicknesses as a function of the electric field. The solid lines represent the results of the model and the corresponding markers represent the measured data. The measured data for the oxides with a thickness of 5.5 and 6.2 nm has been taken from [1]. The hatched line represents the results of the model described in [7], these results are independent of the oxide thickness.

Figure 3 shows the ratio I_p/I_n as a function of the oxide field for different oxide thicknesses. For the parameters B_e in (4) and α in (2) a value of respectively 13.5 and $3.0 \cdot 10^{-5}$ $q(cm^2 \cdot V)^{1/3}$ results in a good agreement between the experimental results and the model. For hot electron injection, a value of $1.0 \cdot 10^{-5}$ $q(cm^2 \cdot V)^{1/3}$ for α is often used[11]. However values of up to $4.0 \cdot 10^{-5}$ $q(cm^2 \cdot V)^{1/3}$ have been reported in literature[16]. A very good agreement between the experimental and the computed results is obtained for all oxide thicknesses with the same set of parameters.

III. Conclusions

A new model for the substrate hole current that occurs during Fowler-Nordheim tunneling is proposed. The model is based on the assumption that hot hole injection occurs at the anode. A very good agreement between the model and the experimental results is obtained for an oxide thickness between 5.5 and 12.5 nm and for electric field strengths in the range of 7-12 MV/cm. The oxide thicknesses that are currently used in nonvolatile memories are within this range. Therefore, since oxide degradation is related to the presence of holes in the oxide, this model can be useful for the modeling of oxide degradation in nonvolatile memories.

Acknowledgements

The authors would like to thank Dr. Masuoka for the helpful discussions and support.

References

1) I.C. Chen, S. Holland, K.K. Young, C. Chang, and C. Hu: Appl. Phys. Lett. 49 (1986) 669.
2) Z.A. Weinberg, M.V. Fischetti, and Y. Nissan-Cohen: J. Appl. Phys. 59 (1986) 824.
3) J.F. Zhang, S. Taylor, and W. Eccleston: J. Appl. Phys. 71 (1992) 725.
4) S. Holland, I.C. Chen, T.P. Ma, and C. Hu: IEEE Electron Device Lett., EDL-5 (1984) 302.
5) I.C. Chen, S. Holland, and C. Hu: IEEE Electron Device Lett. EDL-7 (1986) 164.
6) Z.A. Weinberg and M.V. Fischetti: J. Appl. Phys. 57 (1985) 443.
7) M.V. Fischetti: Phys. Rev. B. 31 (1985) 2099.
8) M.V. Fischetti, D.J. DiMaria, S.D. Brorson, T.N. Theis, and J.R. Kirtley: Phys. Rev. B. 31 (1985) 8124.
9) R.L. Kamocsai and W. Porod: J. Appl. Phys. 69 (1991) 2264.
10) J.P. Nougier, J.C. Vaissiere, D. Gasquet, J. Zimmermann, and E. Constant: J. Appl. Phys. 52 (1981) 825.
11) T.H. Ning: J. Solid-State Electron. 21 (1978) 273.
12) C. Chang, C. Hu, and R.W. Broderson: J. Appl. Phys. 57 (1985) 302.
13) E. Takeda, H. Kume, T. Toyabe, and S. Asai: IEEE Trans. Electron Devices, ED-29 (1982) 611.
14) S.-L. Wang, N. Goldsman, L. Henrickson, and J. Frey: IEDM Tech. Dig. (1990) 447.
15) G.J. Hemink, R.C.M. Wijburg, P.B.M. Wolbert, and H. Wallinga: Proc. of the ESSDERC, (1991) 65.
16) S. Tam, P.-K. Ko, and C. Hu: IEEE Trans. Electron Devices, ED-31 (1984) 1116.